Postprint of the following paper :Fu, S.; Wei, W.; Ou, S.; Moan, T.; Deng, S.; and Lie, H.,(2017), “A time-domain method for hydroelastic analysis of floating bridges in inhomogeneous waves”, ASME 2017 36th International Conference on Ocean, Offshore and Arctic Engineering, Trondheim, Norway.

A TIME-DOMAIN METHOD FOR HYDROELASTIC ANALYSIS OF FLOATING BRIDGES IN INHOMOGENEOUS WAVES

Shixiao Fu
State Key Laboratory of Ocean Engineering,
Shanghai Jiao Tong University, China
SINTEF Ocean, Trondheim, Norway

Wei Wei
State Key Laboratory of Ocean Engineering,
Shanghai Jiao Tong University, China

Shaowu Ou
State Key Laboratory of Ocean Engineering,
Shanghai Jiao Tong University, China

Torgeir Moan
Centre for Ships and Ocean Structures (CeSOS),
Norwegian University of Science and
Technology (NTNU), Trondheim, Norway
Department of Marine Technology,
NTNU, Trondheim, Norway

Shi Deng
Department of Marin Technology
Norwegian University of Science and
Technology, Trondheim, Norway

Halvor Lie
SINTEF Ocean
Trondheim, Norway

ABSTRACT

Based on the three dimensional potential theory and finite element method (FEM), this paper presented a method for time-domain hydroelastic analysis of a floating bridge in inhomogeneous waves. A floating bridge in both regular and irregular waves, is taken as a numerical example. This method is firstly validated by the comparisons of the results between frequency domain method and presented time domain method under regular wave condition. Then the hydroeleastic responses of the floating bridge in waves with spatially varying significant wave height/peak period are presented, with the purpose to illustrate the feasibility of the proposed method. The primary results at this stage indicate that the inhomogeneity of the waves might affect the structure dynamic responses of the floating bridge in waves.

***Key words**:* frequency domain; time domain; hydroelastic analysis; inhomogeneous waves

1. INTRODUCTION

The Norwegian Public Roads Administration (NPRA) is planning to build floating bridges in the fjords to connect the E39. Compared with the traditional underwater tunnel concept, the surface crossing concept is supposed to be economically better. The surface crossing concept is mainly made up by pontoons and bridge girders with a typical crossing distance of 4000 m and become very flexible compared with those of the traditional ocean structures, which is normally named as very large floating structures (VLFS).

VLFS features a larger size while relatively lower structural stiffness and the coupling effect between its structural elastic deformations and wave motions must be considered, which should be solved by hydroelasticity method. Frequency domain hydroelasticity theories have been developed from two-dimensional [1, 2] to three- dimensional [3, 4], from linear [5, 6] to nonlinear [7-9] models.

When it comes to time domain hydroelasticity, normally the Fourier transform method is utilized where the hydrodynamic coefficients by frequency domain analysis are taken as its main inputs [10-12].

On the other hand, based on three dimensional time-domain Green function, and Price-Wu condition [3] at the interface between flexible structures and the surrounding fluid, a direct time domain hydroelasticity method has been developed [13]. Liu and Sakai [14] analyzed the 2D time domain hydroelastic responses of flexible floating structures in regular, random and solitary waves by utilizing BEM for fluid and FEM for structures. Qiu [15] evaluated the dynamic responses of a floating girder under the impulsive and moving loads based on FEM method in a linear system. Although the direct time domain method is beneficial in strong nonlinear problems, it is still time-consuming and requires a large amount of computer resources compared with the Fourier transform method.

In this paper, a time-domain numerical method for the prediction of the hydroelastic responses of the floating bridge in waves is presented by using Fourier transform method. The connecting bridge girder is simulated by equivalent beam stiffness considering Euler-Bernoulli beam

theory together with the St. Venant's torsion theory. By introducing convolution theorem, the frequency-domain wave exciting forces and hydrodynamic coefficients on each pontoon are transformed into the time-domain hydroelastic equation. A floating bridge in both regular and irregular waves, is taken as a numerical example. This method is firstly validated by the comparisons of the results between frequency domain method and presented time domain method under regular wave condition. Then the hydroeleastic responses of the floating bridge under waves with spatially varying significant wave height/peak period are presented.

2. THEORETICAL BACKGROUND

2.1. The coordinate system

Floating pontoons supported continuous bridge girder, from the hydrodynamicsvpoint of view, can be looked as a beam connected multi-floating-body system, and the hydrodynamics can be solved by traditional multi-body hydrodynamic theores. Three right-handed coordinate systems are adopted in this paper to describe the wave-induced motions, which includes global coordinate system *OXYZ* , body-fixed coordinate system $o_m x_m y_m z_m$ and reference coordinate system $o'_m x'_m y'_m z'_m$ as shown in Fig.1. The global coordinate system (*OXYZ*) stays still in space with the *OXY* at still water surface and axis *Z* straight up.

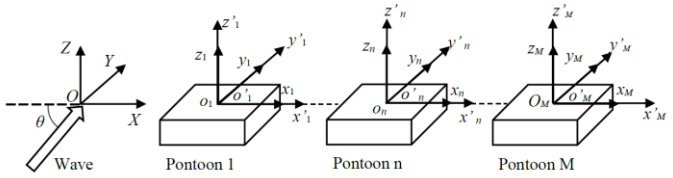

Fig.1 Coordinate system of multiple floating body system

2.2. Motion equations in frequency domain

Based on three dimensional potential theory and linearized Bernoulli equation, the wave excitation forces, added mass and damping coefficients of the multi-body system can be obtained in frequency domain [16]:

$$F_{wj}^{(n)} = \iint_{S_p} pn_j^{(n)} ds = i\rho\omega e^{-i\omega t} \iint_{S_n} (\phi_I + \phi_D) n_j^{(n)} ds \qquad (1)$$

$$A_{kj}^{(nq)} + \frac{iC_{kj}^{(nq)}}{\omega} = \rho \iint_{S_p} \phi_k^{(q)} \frac{\partial \phi_j^{(n)}}{\partial n} dS \qquad (2)$$

where $F_{wj}^{(n)}$ is the j^{th} mode wave excitation force on the n^{th} pontoon; A and C refer to the added mass and damping coefficients, respectively; when $n = q$, they refer to the added mass and damping coefficients caused by the motion of pontoon *n* itself, otherwise they are caused by the motion of other pontoon *q*; *n* and *q* is the number of the pontoons, *k* and *j* is the motion mode number.

The motions of a pontoon will not only be influenced by the hydrodynamic interactions with adjacent pontoons, but also restricted by the motion displacement of adjacent pontoons through the deformations of the connecting beams between them, which ensures the continuous of the whole floating bridge in waves. Under this circumstance, the floating bridge system could be treated as a flexible beam system with concentrating forces from the rigid pontoons acting on the jointing points between the girder and the pontoons along the whole bridge [17]. Then the dynamic motion equations of the elastic beam system with totally N finite element nodes supported by M floating pontoons in waves can be written as,

$$[m]_{6N\times 6N}\{\ddot{x}\}_{6N\times 1} + [D]_{6N\times 6N}\{\dot{x}\}_{6N\times 1} + [k]_{6N\times 6N}\{x\}_{6N\times 1} = \{F\}_{6N\times 1} \qquad (3)$$

where $[m]$ is the mass matrix of the beam system itself, $[D]$ is the structural damping matrix within beam system, $[k]$ is the structural stiffness matrix of the beam, $\{x\}$ is the displacement vector of the nodes of the beam, as shown in Fig.2. $\{F\}$ is the external force vector, which is related to the displacement $\{x\}$ and only has non-zero values on the nodes connecting the girder and the pontoons, as illustrated by Fig.2. In accordance with the potential theory, $\{F\}$ includes the wave excitation force $\{F_w\}$, hydrostatic restoring force $[K]\{x\}$, inertial force of the floating pontoon $[M]\{\ddot{x}\}$ and wave radiation force composed by the added mass force $[A]\{\ddot{x}\}$ and damping force $[C]\{x\}$, where $[K]$ and $[M]$ is the hydrostatic restoring coefficient and mass matrix of the pontoons respectively.

In the above equation, various variables are functions of space and time, $\{x\}$ and $\{F_w\}$ which will periodically vary with stable frequency ω, which can be re-written as,

$$\{x\} = \{\bar{x}\}e^{-i\omega t}, \quad \{F_w\} = \{\bar{f}_w\}e^{-\omega i} \qquad (4)$$

where $\{\bar{x}\}$ is the amplitude of the displacements, and $\{\bar{f}_w\}$ is the wave excitation forces vector with non-zero values on the beam nodes connecting with the pontoons.

Consequently, Eq.(3) can be rewritten by separating time variable:

$$\begin{pmatrix} -\omega^2\left([M+m]_{6N\times 6N}+[A]_{6N\times 6N}\right)-i\omega[C+D]_{6N\times 6N} \\ +[K+k]_{6N\times 6N} \end{pmatrix}\{\bar{x}\}_{6N\times 1} \quad (5)$$
$$=\{\bar{f}_w\}_{6N\times 1}$$

where all of the symbols keep the same meaning as foregoing descriptions.

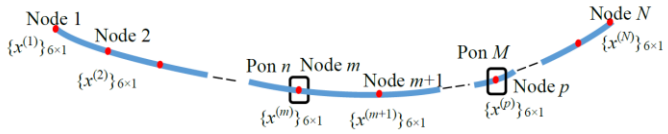

Fig.2 The deformation of the beam

2.3. Motion equations in time domain in inhomogeneous waves

Based on the linear assumption and impulse response function, the time-domain hydrodynamic analysis theory has been established by Cummins [18], which is known as Cummins Equation. For the multi-body system connected by elastic beams, this time-domain motion equations in the global coordinate system can be expressed as:

$$[M+m+A(\infty)]_{6N\times 6N}\{\ddot{x}(t)\}_{6N\times 1}+\int_{-\infty}^{t}[H(t-\tau)]_{6N\times 6N}\{\dot{x}(\tau)\}_{6N\times 1}d\tau$$
$$+[D]_{6N\times 6N}\{\dot{x}(t)\}_{6N\times 1}+[K+k]_{6N\times 6N}\{x(t)\}_{6N\times 1}=\{F_w(t)\}_{6N\times 1} \quad (6)$$

where $[A(\infty)]$ is the added mass coefficient matrix in the infinite wave frequency; $[H(t)]$ is the retardation function matrix; and its integral $\int_{-\infty}^{t}[H(t-\tau)]\{\dot{u}(\tau)\}d\tau$ represents the fluid memory effect; $\{F_w(t)\}$ is the first-order time-domain wave exciting force; just like Eq.(3), the three terms related to waves motions have non-zero values only on the beam nodes connecting with the pontoons; $\{x(t)\},\{\dot{x}(t)\},\{\ddot{x}(t)\}$ are the displacement, velocity and acceleration of the nodes with respect to the inertial reference frame, respectively; other terms have the same meanings as forgoing descriptions.

According to Kramer-Kronig relations based on Fourier transform by Ogilvie [18], the retardation function can be expressed by the frequency results of the added mass or damping coefficients.

$$[H(t)]=-\frac{2}{\pi}\int_0^{\infty}\omega\left([A(\omega)]-[A(\infty)]\right)\sin\omega t d\omega$$
$$=\frac{2}{\pi}\int_0^{\infty}[C(\omega)]\cos\omega t d\omega \quad (7)$$

where $[A(\omega)]$ and $[C(\omega)]$ denote the added masse and damping coefficients in the frequency domain, respectively.

The inhomogeneous wave filed along the floating bridge is divided into p isolated sub-regions. Each sub-region is assumed to be homogeneous, modelled by a 3-parameter JONSWAP spectrum, as shown in Fig.3. And then the wave excitation forces acting on the n^{th} pontoon within k^{th} sub-region could be written as:

$$F_{wj}^{(n)}(t)=\sum_{l=1}^{L}f_{wj}^{(n)}(\omega_l)\sqrt{2S_k(\omega_l)\Delta\omega}\cos\left(\omega t+\varepsilon_l+\beta_j^{(n)}(\omega_l)\right) \quad (8)$$

where the superscript n denotes the n^{th} pontoon, k denotes the k^{th} sub-region, l denotes the l^{th} discrete wave frequency, j denotes the j^{th} mode wave excitation force (j=1,..,6). The same random phase series of ε_l is adopted in different sub-regions. $F_{wj}^{(n)}(t)$ represents the j^{th} DOF wave excitation force on the n^{th} pontoon whose position of sub-region is accordingly allocated according to its coordinates; $\beta_j^{(n)}(\omega_l)$ is the position related phase angle of the wave excitation force on the n^{th} pontoon in the j^{th} mode at wave frequency of ω_l.

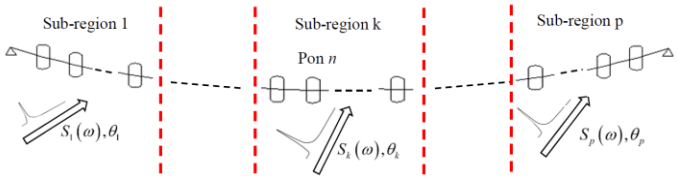

Fig.3 The description of inhomogeneous sea environment

Consequently, the time history of the wave excitation force $\{F_w(t)\}$ in Eq.(6) in an inhomogeneous wave can be expressed in the form of array:

$$\{F_w(t)\}=\left\{...,\{F_{w1}^{(1)}(t)\},...,\{F_{w1}^{(n)}(t)\},...,\{F_{w6}^{(n)}(t)\},...,\{F_{w6}^{(M)}(t)\}...\right\}^T \quad (9)$$

The wave excitation forces on pontoon n have six DOFs and locate on the nodes connecting with the pontoons.

Then Eq.(6) can be solved numerically by Newmark method, and the hydroelastic response in inhomogeneous sea environment can be obtained.

3. NUMERICAL MODEL

The concept of a floating bridge supported by descret pontoons has been proposed in Norway. The bridge girder is a Viererendel beam consisting of two parallel steel boxes spaced sufficiently apart in order to provide adequate bending stiffness about vertical axis and sufficient buckling capacity.

The overall original bridge model is shown in Fig.4, where the bridge girder could be modelled as a single center beam. In this paper, we just choose the right part of the whole

bridge (marked with the red line in Fig.4) as the analysis model, as illustrated in Fig.5, where total 19 floating pontoons with the same geometries are involved along the extension of the bridge girder. The properties of the pontoon are illustrated in Table.1, and the geometry is shown in Fig.6. Two ends of the bridge model are simplified as pin joints as shown in Fig.7.

The connecting beam between each two pontoons has a length of 196.96m, including three segments with different cross sections. The parameters of the first and last section are the same (Section S1) with a length of 24.62m, and the length of the middle section (Section F1) is 147.74m, as listed in Table.1.

Table.1 General Parameters of the Pontoons and Bridge Girder

	Properties	Number	
Bridge Girder	Section	F1	S1
	EA (*kN*)	3.89E8	5.25E8
	EI_y ($kN*m^2$)	2.76E9	3.85E9
	EI_z ($kN*m^2$)	1.55E11	2.18E11
	GI_t ($kN*m^2$)	2.9E9	3.7E9
	Translation Mass (*te/m*)	26.71	31.8
	Rotation Mass ($te*m^2/m$)	8118	10507
Pontoon	Length (*m*)	62	
	Width (*m*)	22	
	Draft (*m*)	10.5	

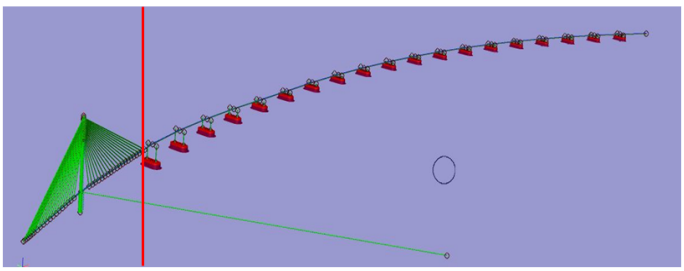

Fig.4 Numerical model for the floating bridge concept [20]

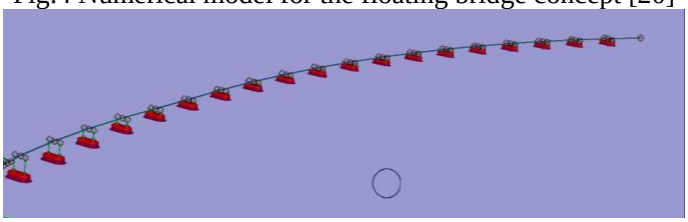

Fig.5 Simplified model

Each pontoon is simplified as a rigid floating body with 6 DOFs. Based on the three dimensional potential theory, the wave exciting forces, added mass and damping coefficients can be directly calculated by panel method in WAMIT in frequency domain. The hydrodynamic interactions between the pontoons are neglected due to the large spacing between them. Fig.6 illustrates the hydrodynamic meshes of the floating pontoon.

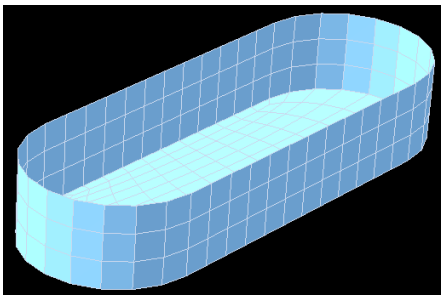

Fig.6 Hydrodynamic Meshes of the Floating Pontoon

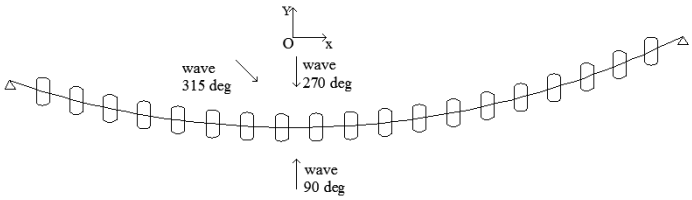

Fig.7 Simplified model

4. RESULTS AND DISCUSSIONS

4.1. Results obtained from frequency-domain method

To be concrete, distributions of the vertical displacement, horizontal displacement and torsional angle along the floating bridge under a regular wave of 0.6 rad/s are presented in Fig.8, all of which are derived from frequency domain method. Obviously, due to the non-symmetrical distribution of forces on the pontoons, the displacements of the bridge are causally not symmetrical along the longitudinal direction as well. As shown in Fig.8 (a), the maximum vertical displacement under inside waves (270deg wave direction) is slightly larger than that under outside waves (90deg wave direction). Similar tendencies can be discovered in Fig.8 (b) and Fig.8 (c). There are also some evident differences for different positions along the bridge, which are induced by different wave phases on pontoons and the continuity of the deformation owing to the connecting beams.

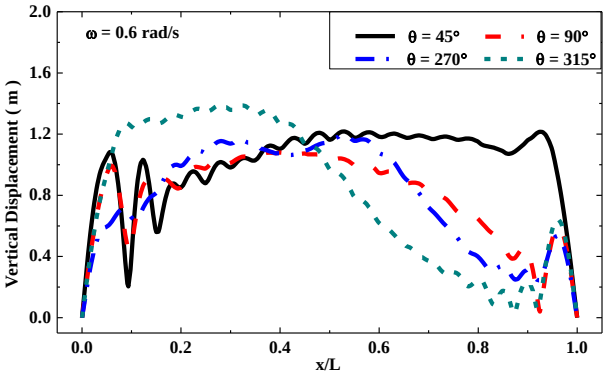

(a) Vertical displacement

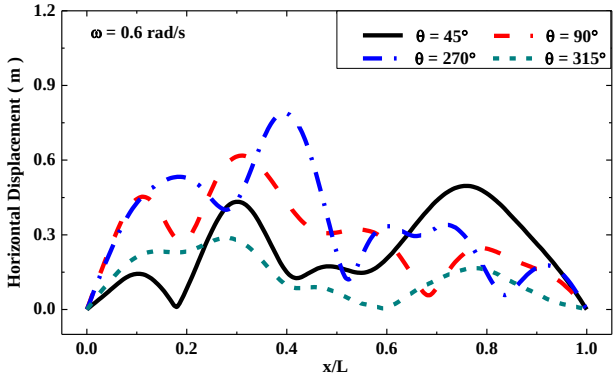

(b) Horizontal displacement

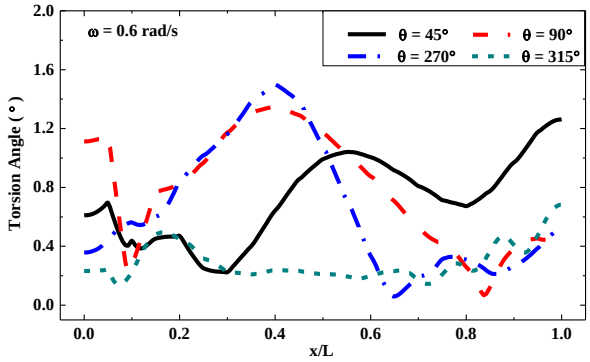

(c) Torsion angle

Fig.8 The displacement of the floating bridge in the wave frequency of 0.6rad/s for different wave directions.

4.2. Time-domain responses in regular waves

In the time-domain simulation in regular waves, the time history of the first order wave exciting force can be obtained based on the amplitudes and phase angles of the wave exciting force in frequency domain, and it can be described as:

$$F_w(t) = \bar{F}_w \cos(\omega t + \phi) \tag{10}$$

where $\bar{F}_{w1}$ denotes the amplitude of the wave exciting force obtained in frequency domain; ϕ is the corresponding phase angle. In the numerical simulation, the time step is 0.1s and the initial displacement and initial velocity of the pontoons are both zero.

Given the amplitudes and phase angles of wave exciting forces, responses obtained from the direct time-domain numerical simulation and those transformed from frequency domain ought to agree well with each other. It is an approach to validate the proposed method. Fig.9 illustrated the time history of the vertical displacement at the middle of the bridge under the regular wave with a frequency of $0.6rad/s$ and a direction of 90°. As can be seen, after a period of time, the response will become stable in terms of the amplitude in time domain results. And the amplitudes shown in time history are found to match well with the harmonic vertical displacement from frequency domain method. Therefore, the proposed time-domain hydroelastic method is validated.

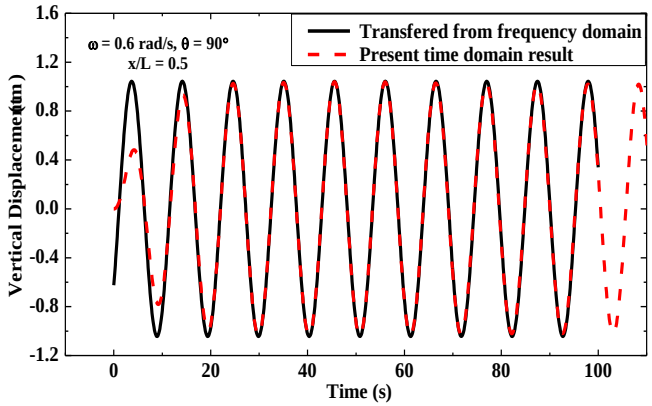

Fig.9 Time series of vertical displacement in the wave frequency $\omega = 0.3rad/s$ in the wave direction of 90°.

The transformation method used in this paper is based on FFT theory and it also needs to be validated. Fig.10 illustrates the comparison between the direct frequency-domain results and the results transformed from the time series. It can be found that two curves agree well, indicating that the reliability of present time domain method.

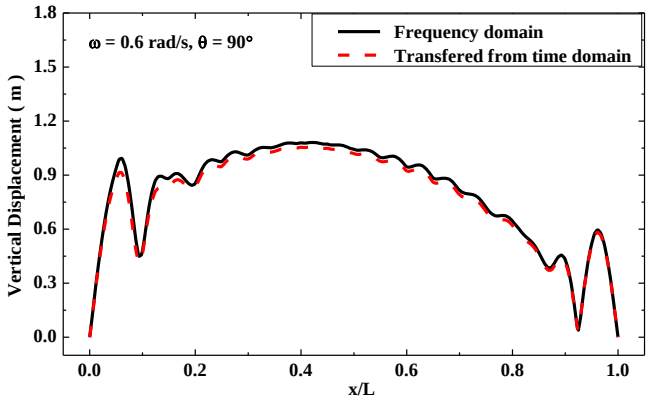

(a) Vertical displacement

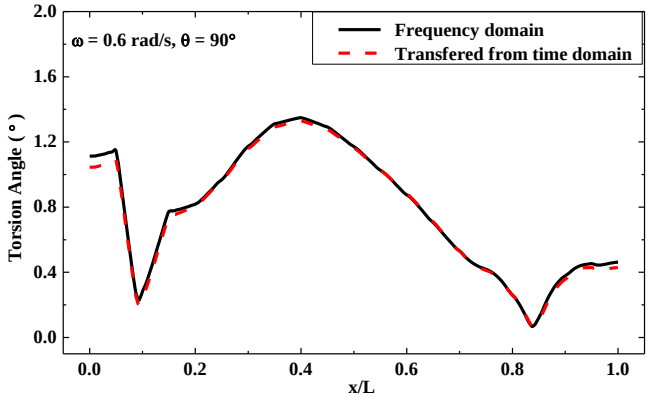

(b) Torsion Angle

Fig.10 The vertical displacement and torsion angle along the longitudinal direction for $\omega = 0.6 rad/s$ in the wave direction of 90 °.

4.3. Time-domain responses in inhomogeneous irregular waves

In this paper, the inhomogeneous wave field is divided into 4 sub-regions. The irregular wave parameters at each sub-region along the floating bridge are displayed in Table.2 and Fig.11.

Table.2 Wave Parameters at each sub-region along the bridge length [19]

Env. Number	Regions(from West to East)	Significant wave height(H_s/m)	Peak period(T_p/s)
Env.1	Region A (0-1km)	2.0	5
Env.2	Region B (1-2km)	1.9	6
Env.3	Region C (2-3km)	2.4	7.5
Env.4	Region D (3-4km)	2.8	8.5

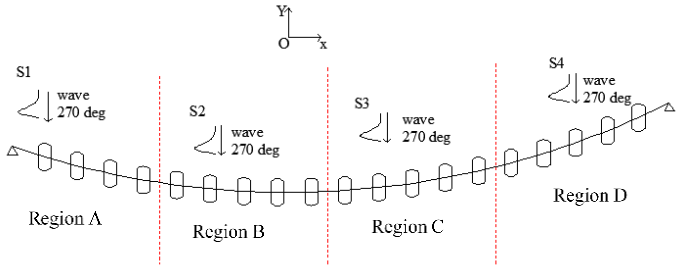

Fig.11 Distribution of inhomogeneous wave field

Irregular wave time series in each sub-region is generated from the defined wave spectrum ranging from 0.1 to 3rad/s in each sub-region. For all of the four irregular waves, wave frequencies and random phase angles are kept constant to guarantee the continuity of wave field. In addition, the wave frequency is randomly distributed to avoid the periodical repetition of the generated wave elevations.

Fig.12 shows the comparisons of the significant values of the vertical displacement, horizontal displacement and torsion angle along the longitudinal direction between the inhomogeneous wave and the homogeneous waves for the wave direction of 270 °. The boundaries between each sub-region have been marked by lines as shown in the figures. As can be seen, the responses along the longitudinal direction in inhomogeneous waves are always smaller than that in homogeneous wave with the maximum wave height of *Hs*=2.8*m*, especially in region A, B and C, where the significant wave height is smaller than 2.8m. In region B, the vertical displacement of the pontoon near region C is obviously larger than those pontoons in region B, which is due to the continuous conditions of the displacements. The horizontal displacement and torsion angle are rather smaller in the inhomogeneous wave, indicating that the inhomogeneous effect is not obvious on the torsional deformations.

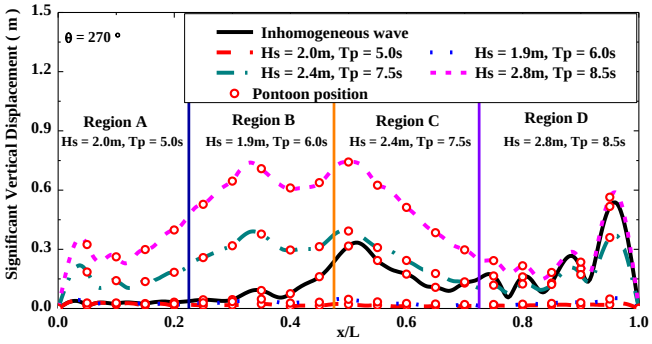

(a) Vertical displacement for θ=270°

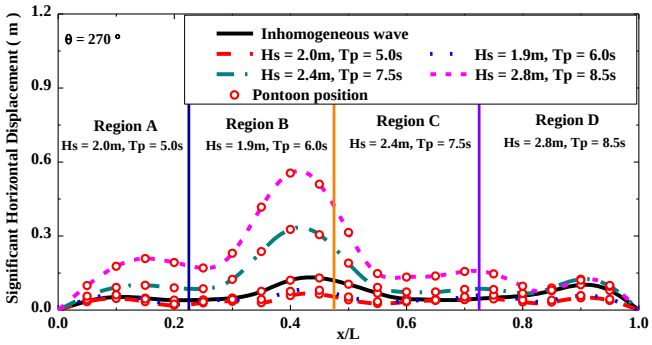

(b) Horizontal displacement for θ=270°

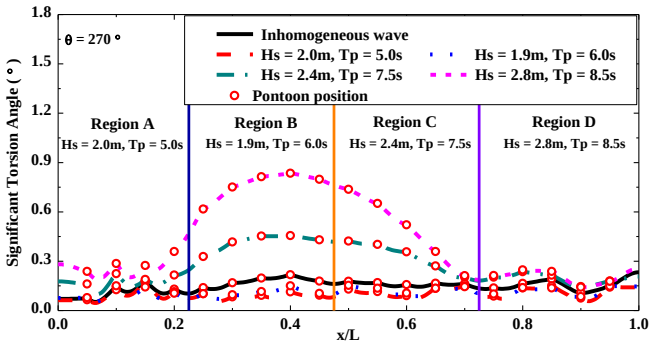

(c) Torsion angle for θ=270°

Fig.12 The significant displacements along the longitudinal direction in the homogenous and inhomogeneous waves for the wave direction of 270 °.

The distribution of the vertical bending moment, horizontal bending moment and torsion of each connected beam between the two pontoons under their local coordinate systems along the floating bridge are illustrated in Fig.13. It can be found that the maximum vertical bending moment on each segment always appears around the positions of pontoons. Similar with the trends of displacements, the vertical bending moment, the horizontal bending moment and torque in the inhomogeneous waves are always smaller than those in the highest homogeneous wave of *Hs*=2.8*m*. The maximum horizontal bending moment in homogeneous wave of *Hs*=2.8*m* is almost 3 times of those in the inhomogeneous wave for some positions.

Consequently, as for the wave loads applied to the floating pontoons, if the highest wave parameters are adopted, the bending moments of the structure will be over-estimated. If the lowest homogeneous wave parameters are adopted, safety design cannot be guaranteed. Therefore, wave inhomogeneity should be taken into account in the bridge design.

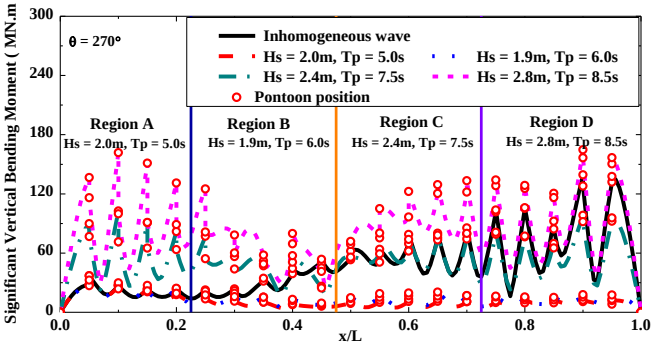

(a) Vertical bending moment for θ=270°

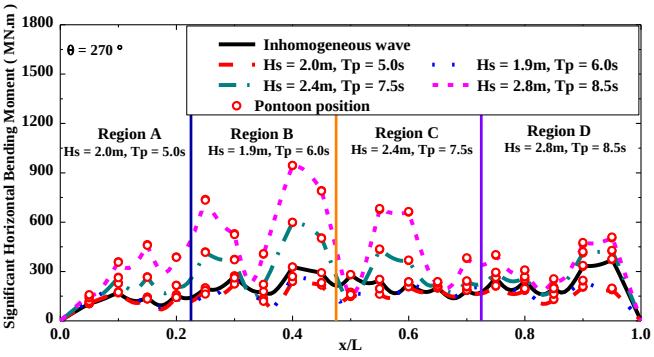

(b) Horizontal bending moment for θ=270°

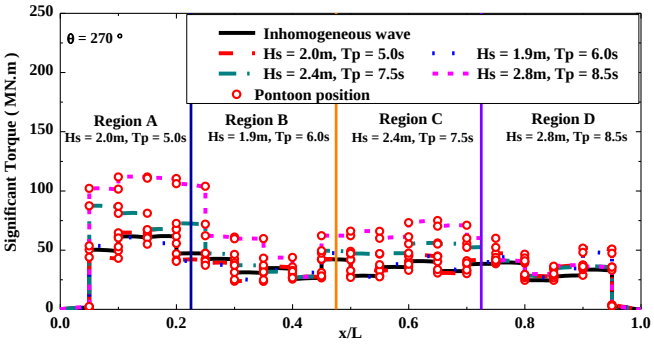

(c) Torsion for θ=270°

Fig.13 The significant moments of each connected beam in their local coordinate system in the homogenous and inhomogeneous waves for the wave direction of 270 °.

5. CONCLUDING REMARKS

A time-domain approach is proposed for hydroelastic analysis of a curved floating bridge in inhomogeneous wave conditions. The method is firstly validated against frequency-domain results，and then applied to investigate the effect of the inhomogeneous waves on the hydroelastic responses a curved floating bridge, including both spatial varying wave heights/periods and incident wave directions. The results show that the inhomogeneity of the waves might have effects on the dynamic responses of a floating bridge. The responses will be greatly overestimated if only the maximum homogeneous wave conditions are used as the environment input, while it cannot guarantee a safe design if only the small homogeneous wave is applied.

This paper is mainly focusing on the validation and feasibility of the newly developed methods. The inhomogeneous waves used are measured data from another fjord in Norway [19], not specifically for the current floating bridge site. Regarding the effect of the inhomogeneity of the waves, further studies need to be carried out to make more general conclusions.

REFERENCE

[1]Betts, Bishop, R., & Price, W., 1977. The symmetric generalised fluid forces applied to a ship in a seaway. RINA Supplementary Papers, 119.

[2] Bishop, R., Price, W., & Temarel, P., 1979. A unified dynamical analysis of antisymmetric ship response to waves.

[3] Wu, Y., 1984. Hydroelasticity of floating bodies. University of Brunel.

[4] Chen, X., Moan, T., Fu, S., & Cui, W., 2005. Hydroelastic analysis of flexible floating structures in regular waves. Paper presented at the Proceedings of the International Conference on Mechanical Engineering and Mechanics, ICMEM.

[5] Wu, Y., Wang, D., Riggs, H. R., & Ertekin, R. C., 1993. Composite singularity distribution method with application to hydroelasticity. Marine Structures, 6(2-3), 143-163.

[6] Fu, S., Moan, T., Chen, X., & Cui, W., 2007. Hydroelastic analysis of flexible floating interconnected structures. Ocean Engineering, 34(11), 1516-1531.

[7] Chen, X., Wu, Y., Cui, W., & Tang, X., 2003. Nonlinear hydroelastic analysis of a moored floating body. Ocean Engineering, 30(8), 965-1003.

[8] Chen, X., Moan, T., Fu, S., & Cui, W., 2006. Second-order hydroelastic analysis of a floating plate in multidirectional irregular waves. International Journal of Non-Linear Mechanics, 41(10), 1206-1218.

[9] Chen, X., Moan, T., & Fu, S., 2010. Extreme response of Very Large Floating Structure considering second-order hydroelastic effects in multidirectional irregular waves. Journal of Offshore Mechanics and Arctic Engineering, 132(4), 041601.

[10] Taghipour, R., Perez, T., & Moan, T., 2008. Hybrid frequency–time domain models for dynamic response analysis of marine structures. Ocean Engineering, 35(7), 685-705.

[11] Kashiwagi, M., 2000. A time-domain mode-expansion method for calculating transient elastic responses of a pontoon-type VLFS. Journal of marine science and technology, 5(2), 89-100.

[12] Kashiwagi, M., 2004. Transient responses of a VLFS during landing and take-off of an airplane. Journal of marine science and technology, 9(1), 14-23.

[13] Wang, D.-Y., and Wu, Y.-S., 1998. Three-dimensional hydroelastic analysis in time domain with application to an elastic ship model. JOURNAL OF HYDRODYNAMICS SERIES B-ENGLISH EDITION-, 10, 54-61.

[14] Liu, X., & Sakai, S., 2002. Time domain analysis on the dynamic response of a flexible floating structure to waves. Journal of engineering mechanics, 128(1), 48-56.

[15] Qiu, L.-c., 2007. Numerical simulation of transient hydroelastic response of a floating beam induced by landing loads. Applied ocean research, 29(3), 91-98.

[16] Løken, A., 1981. Hydrodynamic interaction between several floating bodies of arbitrary form in waves. HYDRODYNAMICS IN OCEAN ENGINEERING,(198, 745-759.

[17] Wei, W., Fu, S., Moan, T., Deng, S., Lu, Z., 2016. A discrete-modules-based hydroelasticity method for floating structures in finite water depth with even and uneven sea bottom, submitted to Journal of Fluids and Structures, YJFLS_2016_522.

[18] Ogilvie, T. F., 1964. Recent progress toward the understanding and prediction of ship motions. Paper presented at the 5th Symposium on naval hydrodynamics.

[19] Lie, H., Fu, S., Fylling, I., Fredriksen, A. G., Bonnemaire, B., and Kjersem, G. L., "Numerical Modelling of Floating and Submerged Bridges Subjected to Wave, Current and Wind," Proc. ASME 2016 35th International Conference on Ocean, Offshore and Arctic Engineering, American Society of Mechanical Engineers, pp. V007T006A075-V007T006A075.

[20] Curved Bridge South – Environmental Loading Analysis - Input to Norwaframe and OrcaFlex, 2016, Report from Norwegian Public Roads Administration.